OPEN ACCESS

International
Journal
Of Modern Engineering Research (IJMER)

Resolution of human arm redundancy in point tasks by synthesizing two criteria

Kashi Barak[1], Li Zhi[2], Rosen Jacob[3], Avrahami Idit[4], Brand Moshe[5]

[1](*School of Mechanical Engineering, Tel-Aviv University, Israel)*
[2,3](*Department of Computer Engineering, University of CaliforniaSanta Cruz,USA)*
[4,5](*Department of Mechanical Engineering and Mechatronics, Ariel University, Israel)*

Abstract: *The human arm is kinematically redundant in the task of pointing. As a result, multiple arm configurations can be used to complete a pointing task in which the tip of the index finger is brought to a preselected point in a 3D space. The authors have developed a four degrees of freedom (DOF)model of the human arm with synthesis of two redundancy resolution criteria that were developed as an analytical tool for studying the positioning tasks. The two criteria were: (1) minimizing the angular joint displacement (Minimal Angular Displacement - MAD) and (2) averaging the limits of the shoulder joint range (Joint Range Availability - JRA). As part of the experimental protocol conducted with ten subjects, the kinematics of the human arm was acquired with a motion capturing system in a 3D space. The redundant joint angles predicted by a equally weighted model synthesizing the MAD and JRA criteria resulted with a linear correlation with the experimental data (slope=0.88; offset=1°; r^2=0.52). Given the experiment protocol, individual criterion showed weaker correlation with experimental data (MAD slope=0.57, offset=14°, r^2=0.36 or JRA slope=0.84, offset=-1°, r^2=0.45). Solving the inverse kinematics problem of articulated redundant serials mechanism such as a human or a robotic arm has applications in fields of human-robot interaction and wearable robotics, ergonomics, and computer graphics animation.***

Keywords: *human arm, redundancy, pointing task, kinematics, optimization.*

I. INTRODUCTION

Pointing with the fingertip to a preselected point in space is a task that involves three degrees of freedom (DOF), which arethe X,Y and Z coordinates of the point in space.The human arm includes seven DOF excluding scapular motion. When the wrist joint is fixed, four DOF ($\theta, \eta, \zeta, \phi$ - Fig. 1a) remain active. Since the number of DOF of the arm is greater than the number of DOF required for the pointing task, the arm is considered a redundant manipulator. As such, a specific pointing task can be accomplished by infinite arm configurations. As a result, there is not a unique solution for the inverse kinematics (IK) problem involved in defining the joint angles of the human arm given a pointing task.

Despite the human arm redundancy, it has been shown experimentally that a small range of unique solutions for the joint angles are selected by human subjects in pointing tasks, a result consistent within and across multiple participants[1-5]. It has also been shown experimentally that the final arm configuration depends on its initial posture [2-5]. One approach for solving the under-determined IK problem of the redundant human arm is by adding additional kinematics, dynamics, or energy-based criteria, formulated as a cost functions. As part of the solution, the cost function is either minimized or maximized to provide a unique solution to the IK problem when applied to intermediate points along the trajectory of the human arm end effector (i.e. the finger tip for a point task)[3-10].

Optimization criteria may be divided into two classes: (1) biomechanical (kinematics and dynamics of the human body) criteria and (2) anatomical based criteria. The first class includes the minimal angular displacement (MAD) model[3,4], the minimal work model [3,5], the minimal peak kinetic energy model[4], the minimal torque change model[5,6] and the minimal potential energy change model [8]. Physical quantities such as energy, torque or displacement form the cost function which is further minimized or maximized as part of the solution. The second class is based on anatomical models such as the joint range availability (JRA) criterion (also called Dexterity) [7] and the minimum discomfort criterion[9]. The cost functions in this class are based on anthropometric data of joint motion ranges, the intension of which is to quantify psychophysical discomfort related to the proximity to joint limits or nominal arm configuration.

The majority of these models, when studied individually, and validated experimentally, have demonstrated limited capabilities for solving the IK problem of a redundant human arm and predicting arm

onfiguration. In order to overcome the limited capabilities of individual criteria, it was suggested that two or more criteria should be synthesized with weighted factors [3-5], [12-14].

II. MATERIALS AND METHODS

2.1 Kinematic Arm Model

The human arm may be modeled as aserial kinematic chain. For the purposes of this study it is modeled as a four DOF kinematic linkage, consisting of two links (upper arm and forearm along with the hand) and two joints (shoulder joint and elbow joint, wherethe wrist joint is fixed). The shoulder joint is simplified as a ball and socket joint with three DOFs, and the elbow is simplified as a revolute joint with a single DOF. This model implies that the forearmand hand are aligned with a fixed wrist jointangle during a reach and point movement.

While the position of the hand in Cartesian space is defined by three coordinates (x,y,z), the posture of the arm requires four angles to fully and uniquely specify its configuration.As a result the human arm model may be treated as a kinematically redundant mechanism with respect toa pointing task[15].

2.1.1 Forward Kinematics

The forward kinematics equations of a 4 DOF human arm model (see Fig. 1a and Fig. 1b) are defined by (1) - (4) for which $\theta$is the pitch angle, $\eta$is the yaw angle, $\zeta$is the upper arm torsion angle (shoulder joint), and $\phi$is the flexion/exertion angle of the elbow joint.

$$\begin{bmatrix} {}^{0}\boldsymbol{P}_{e} \\ 1 \end{bmatrix} = \begin{bmatrix} {}^{0}\boldsymbol{T}_{s} \end{bmatrix} \cdot \begin{bmatrix} {}^{s}\boldsymbol{P}_{e} \\ 1 \end{bmatrix} \tag{1}$$

$$\begin{bmatrix} {}^{0}\boldsymbol{P}_{f} \\ 1 \end{bmatrix} = \begin{bmatrix} {}^{0}\boldsymbol{T}_{s} \end{bmatrix} \cdot \begin{bmatrix} {}^{s}\boldsymbol{T}_{e} \end{bmatrix} \cdot \begin{bmatrix} {}^{e}\boldsymbol{P}_{f} \\ 1 \end{bmatrix} \tag{2}$$

where ${}^{0}\boldsymbol{P}_{f} = (x_f, y_f, z_f)^{T}$ and ${}^{0}\boldsymbol{P}_{e} = (x_e, y_e, z_e)^{T}$ are the elbow and fingertip position vectors in a shoulder fixed frame, ${}^{e}\boldsymbol{P}_{f} = (0,0,-L_2)^{T}$ is the fingertip position vector in an elbow frame, ${}^{e}\boldsymbol{P}_{f}$ is the elbow's position in a shoulder frame, L_2 is the distance from the elbow to the fingertip, ${}^{0}\boldsymbol{T}_{s}$ and ${}^{s}\boldsymbol{T}_{e}$ are the 4x4 homogenous transformation matrices for the shoulder and elbow joints, respectively, as defined by (3) and (4):

$${}^{0}\boldsymbol{T}_{s} = \boldsymbol{T}_{z}(\zeta)\cdot\boldsymbol{T}_{x}(\theta)\cdot\boldsymbol{T}_{z}(\eta) = \begin{bmatrix} C\zeta & S\zeta & 0 & 0 \\ -S\zeta & C\zeta & 0 & 0 \\ 0 & 0 & 1 & 0 \\ 0 & 0 & 0 & 1 \end{bmatrix} \cdot \begin{bmatrix} 1 & 0 & 0 & 0 \\ 0 & C\theta & -S\theta & 0 \\ 0 & S\theta & C\theta & 0 \\ 0 & 0 & 0 & 1 \end{bmatrix} \cdot \begin{bmatrix} C\eta & S\eta & 0 & 0 \\ -S\eta & C\eta & 0 & 0 \\ 0 & 0 & 1 & 0 \\ 0 & 0 & 0 & 1 \end{bmatrix} \tag{3}$$

$${}^{s}\boldsymbol{T}_{e} = \boldsymbol{T}_{x}(\phi)\cdot\boldsymbol{T}(0,0,-L_2) = \begin{bmatrix} 1 & 0 & 0 & 0 \\ 0 & C\phi & -S\phi & 0 \\ 0 & S\phi & C\phi & 0 \\ 0 & 0 & 0 & 1 \end{bmatrix} \cdot \begin{bmatrix} 1 & 0 & 0 & 0 \\ 0 & 1 & 0 & 0 \\ 0 & 0 & 1 & -L_1 \\ 0 & 0 & 0 & 1 \end{bmatrix} \tag{4}$$

where $\boldsymbol{T}_x$ and $\boldsymbol{T}_z$ are 4x4 Homogeneous transformation matrices (pure rotations), $\boldsymbol{T}$ is a 4x4 coordinate translation matrix, and L_1 is the distance from the shoulder to the elbow.

Once the position of the hand is fixed at a specific target in space, the elbow joint may swivel around a virtual line connecting the shoulder joint and the location of the hand with an angle defined as the swivel angle αwhich constitutes the redundancy of the human arm (see Fig. 1c). Given the physiological joint limits, the elbow joint may only follow a limited arc out of the full circle depicted in Fig. 1b.

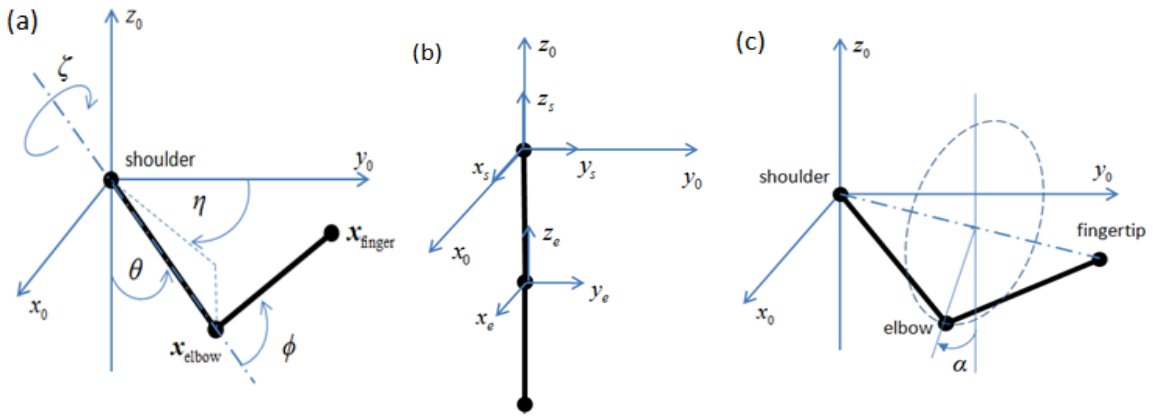

Figure 1:A 4 DOF model of the human arm: (a) Shoulder and elbow joints coordinate systems.(b) The swivel angle α. (c) Definition of arm parameters – shoulder joint pitch angle θ, yaw angle η, torsion angle ζ and elbow joint flexion/extension angle ϕ.

By solving (1) for ${}^{0}\boldsymbol{P}_{\mathrm{f}}$, we obtain:

$$x_{\mathrm{f}} = -L_1 \mathrm{Sin}\,\eta \,\mathrm{Sin}\,\theta - L_2 \mathrm{Sin}\,\phi\left(\mathrm{Cos}\,\zeta\,\mathrm{Sin}\,\eta\,\mathrm{Cos}\,\theta + \mathrm{Sin}\,\zeta\,\mathrm{Cos}\,\eta\right) + L_2 \mathrm{Cos}\,\phi\,\mathrm{Sin}\,\eta\,\mathrm{Sin}\,\theta \tag{5}$$

$$y_{\mathrm{f}} = L_1 \mathrm{Cos}\,\eta\,\mathrm{Sin}\,\theta + L_2 \mathrm{Sin}\,\phi\left(\mathrm{Cos}\,\zeta\,\mathrm{Sin}\,\eta\,\mathrm{Cos}\,\theta + \mathrm{Sin}\,\zeta\,\mathrm{Sin}\,\eta\right) + L_2 \mathrm{Cos}\,\phi\,\mathrm{Sin}\,\eta\,\mathrm{Sin}\,\theta \tag{6}$$

$$z_{\mathrm{f}} = -L_1 \mathrm{Cos}\,\theta + L_2\left(\mathrm{Sin}\,\phi\,\mathrm{Cos}\,\zeta\,\mathrm{Sin}\,\theta - \mathrm{Cos}\,\phi\,\mathrm{Cos}\,\theta\right) \tag{7}$$

2.1.2Inverse Kinematics (IK)

One may note that the FK defines the fingertip position (x,y,z) as a function of the four angles of the arm θ, η, ζ *and* ϕ. For solving the IK, given the fingertip position and the redundancy of the mechanism, the problem is underdetermined. There are 4 unknowns (θ, η, ζ *and* ϕ) and only 3 equations (5-7). To obtain a closed form solution one of the unknowns must be specified. Alternatively, the IK problem can be formulated by using the swivel angle (8) or by defining the elbow joint position (9). These two alternative approaches were used to solve the IK namely the arm configuration $\boldsymbol{\Theta}=(\theta,\eta,\zeta,\phi)^{\mathrm{T}}$:

$$\boldsymbol{\Theta} = \left(\boldsymbol{P}_{\mathrm{f}}, \alpha\right) \tag{8}$$

$$\boldsymbol{\Theta} = \left(\boldsymbol{P}_{\mathrm{f}}, \boldsymbol{P}_{\mathrm{e}}\right) \tag{9}$$

where $\boldsymbol{P}_{\mathrm{e}} = \left(x_{\mathrm{e}}, y_{\mathrm{e}}, z_{\mathrm{e}}\right)^{\mathrm{T}}$.

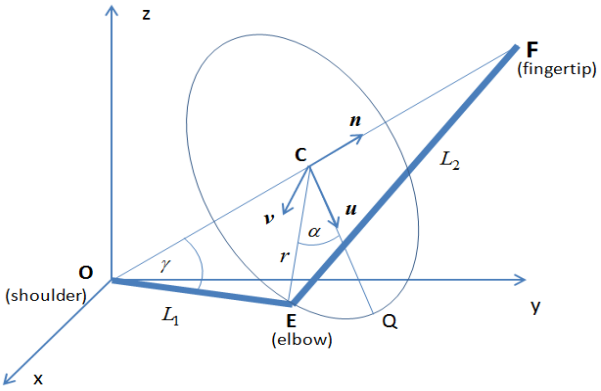

Figure 2: Definition of a local coordinate system at the center of the swivel circle, the point Q and the angle γ.

In order to find the arm's posture, given a swivel angle, first, the elbow's position is defined first. A virtual line is defined connecting the center of the shoulder joint and the fingertip. This line is depicted in Fig. 2 as the swivel axis $\overline{\mathrm{OF}}$. A plane perpendicular to this line intersects with the line a point C and with the center of the elbow joint at point E. The swivel circle is formed at this plane with a center at point C with a radius *r*. A local coordinate system is define with the origin at the center of the circle at point C and three unit vectors ***u***,***v***, and **n** such that ***u***is pointing down along the vector of gravity, ***v*** is located at the same plane but perpendicular to ***u***, and ***n*** is perpendicular to the plane. The three unit vectors are defined in mathematically as :

$$\boldsymbol{n} = \frac{\boldsymbol{P}_{\mathrm{f}}}{\left\|\boldsymbol{P}_{\mathrm{f}}\right\|} \tag{10}$$

$$\boldsymbol{u} = \frac{-\boldsymbol{z} + (\boldsymbol{z}\cdot\boldsymbol{n})\boldsymbol{n}}{\left\|-\boldsymbol{z} + (\boldsymbol{z}\cdot\boldsymbol{n})\boldsymbol{n}\right\|} \tag{11}$$

$$\boldsymbol{v} = \boldsymbol{u}\times\boldsymbol{n} \tag{12}$$

where ***z*** is a unit vector with the direction of the *z* axis as defined in Fig. 1a. We also define the angle $\gamma = \angle\mathrm{FOE}$ and calculate it as in:

$$\gamma = \mathrm{Cos}^{-1}\frac{\left\|\overline{\mathrm{OF}}\right\| - L_1^2 - L_2^2}{2L_1L_2} \tag{13}$$

The center of the swivel circle is defined by:

$$\overline{\mathrm{OC}} = \boldsymbol{n}L_1\mathrm{Cos}\gamma \tag{14}$$

and the radius of the circle is defined by:

$$r = \sqrt{L_1^2 - \left\|\overline{\mathrm{OC}}\right\|^2} \tag{15}$$

The elbow's position $\boldsymbol{P}_e = \overline{\mathrm{OE}}$ can now be obtained by:

$$\overline{\mathrm{OE}} = \overline{\mathrm{OC}} + r\left(\boldsymbol{u}\mathrm{Cos}\alpha + \boldsymbol{v}\mathrm{Sin}\alpha\right) \tag{16}$$

The 4 DOF angles are calculated using trigonometric relations as follows:

$$\theta = \mathrm{Cos}^{-1}\frac{-Z_e}{L_1} \tag{17}$$

$$\eta = \mathrm{Atan2}\left(-x_e, y_e\right) \tag{18}$$

$$\zeta = \mathrm{Atan2}\left(L_1\left(x_e y_f - x_f y_e\right), y_e\left(y_e z_f - y_f z_e\right) - x_e\left(z_e x_f - z_f x_e\right)\right) \tag{19}$$

$$\phi = \pi - \mathrm{Cos}^{-1}\frac{x_f^2 + y_f^2 + z_f^2 + L_1^2 + L_2^2}{2L_1L_2} \tag{20}$$

To find the arm's posture, given an elbow position, one may notice that:

$$\overline{\mathrm{OQ}} = \overline{\mathrm{OC}} + r\boldsymbol{u} \tag{21}$$

and then:

$$\alpha = \frac{\overline{\mathrm{CE}}\cdot\boldsymbol{v}}{\left\|\overline{\mathrm{CE}}\cdot\boldsymbol{v}\right\|}\mathrm{Cos}^{-1}\frac{\overline{\mathrm{CE}}\cdot\overline{\mathrm{CQ}}}{\left\|\overline{\mathrm{CE}}\cdot\overline{\mathrm{CQ}}\right\|} \tag{22}$$

Note that none of these procedures provide a solution to the IK problem of the kinematically redundant mechanisms, because either swivel angle, or elbow position is required.

2.2 Shoulder and elbow joints motion range

An experimental model was previously developed which predicts the shoulder complex range of motion [16]. This model defines the shoulder sinus cone, which restricts the angular motion of the shoulder joint's pitch and yaw angles as depicted in Fig. 3a.

The humeral torsionmotion range was found to be dependent on the former two angles depicted in Fig 3b using a model based on experimental data [17]. The maximal internal and external upper arm torsion surfaces were fitted into a polynomial function. Fig. 4 shows the upper and lower limits of the torsion range of motion.The motion range of the elbow joint (flexion/extension angle) is bounded by a minimal and a maximal value as defined by $\phi_{\min} < \phi < \phi_{\max}$. Since the elbow flexion/extension angle is uniquely defined by the distance between the center of the shoulder joint and the hand, it can be calculated directly according to the hand's position and the segments' lengths.

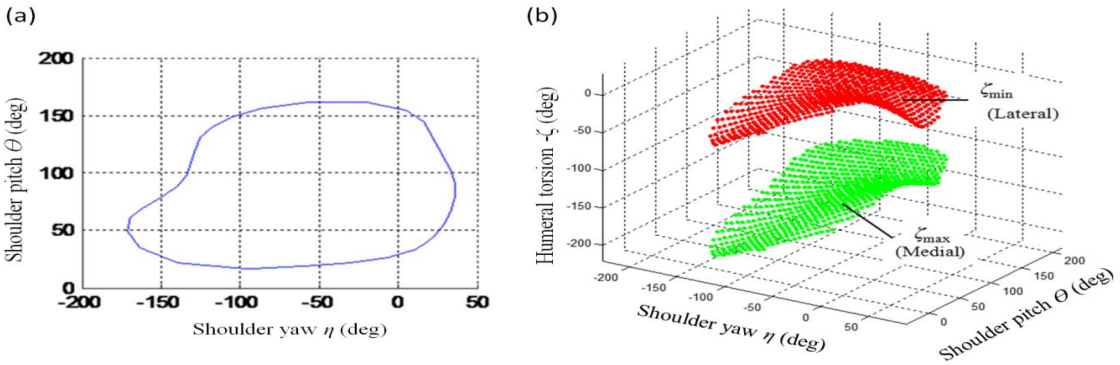

Figure 3: (a) Shoulder joints' dependencies on pitch and yaw angles. (b) Upper (red) and lower (green) limits of humeral torsion. The distance between the two surfaces defines the torsion motion range.

Using this model, we can define a valid posture of the human arm to be a posture that complies with the conditions in (23):

$$\begin{cases} \theta_{\min}(\eta) < \theta < \theta_{\max}(\eta) \\ \eta_{\min}(\theta) < \eta < \eta_{\max}(\theta) \\ \zeta_{\min}(\theta,\eta) < \zeta < \zeta_{\max}(\theta,\eta) \end{cases} \tag{23}$$

An alternative and simpler approach to the shoulder's joint motion range is given by constant ranges to each DOF, independent on each other. Values for joint limits can be found in anthropometric data sources [18] as in (24):

$$\begin{cases} 0 < \theta < 180° \\ -134° < \eta < 48° \\ -34° < \zeta < 97° \end{cases} \tag{24}$$

Both approaches are used in this study, in order to compare their effect on the solution of the kinematic redundancy problem of the human arm.

2.3 Joint Range Availability (JRA) Criterion

The JRA criterion is based on the assumption that the human arm tends to adopt postures with joint angles that are as close as possible to their mid-range values and as far as possible from their joint limits. As the elbow joint swivels, and (theoretically) provides an infinite number of possible arm postures (solutions to the IK problem), the pitch, yaw and torsion angles of the shoulder joint are adjusted appropriately to maintain the hand position. A valid anatomical posture is achieved if all three angles of the shoulder joint are within their anatomical ranges of motion either according to (23) or according to (24).There is a continuous subset of valid arm postures with a swivel angle in the range of $\alpha_{\min} < \alpha < \alpha_{\max}$. Based on the JRA criterion, the optimal posture is achieved by a mean value of the swivel angle limits defined by:

$$\alpha_{\text{mean}} = \frac{\alpha_{\min} + \alpha_{\max}}{2} \tag{25}$$

Figure 4 illustrates the swivel angle limits and the optimal posture at some handposition in space.

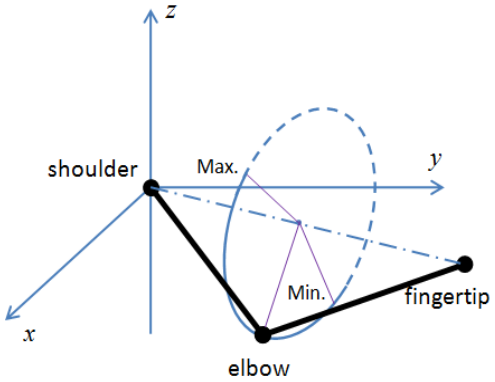

Figure 4: Swivel angle limits and optimal posture. The solid arc denotes valid postures domain. Dashed arc denotes invalid postures domain.

2.4Minimal Angular Displacement Criterion (MAD)

The minimal angular displacement (MAD) criterion minimizes the sum of the differences of the various joint angles, between their initial and final values. In other words, the final arm posture defined by this criterion yields the shortest distance between the initial and the final value of the joint angles in joint space. This criterion can be formulated as an optimization problem using the following cost function:

$$f_{\text{MAD}} = \left(\theta^{\text{f}} - \theta^{\text{i}}\right)^2 + \left(\eta^{\text{f}} - \eta^{\text{i}}\right)^2 + \left(\zeta^{\text{f}} - \zeta^{\text{i}}\right)^2 \tag{26}$$

where i denotes initial value and f denotes final value for the pitch, yaw, and torsion angles. However, it has been shown experimentally that the shoulder joint velocities vary simultaneously [4]. Therefore, the shoulder shifts directly from its initial pitch and yaw angles to its final pitch and yaw angles (see Fig. 5), and not by two separate rotations as implied by (26). This rotation occurs about an axis that is normal to the plane formed by the shoulder (**O**), the initial elbow position ($\mathbf{P}_1$), and the elbow final position ($\mathbf{P}_2$). The direct rotation of the shoulder, and the direct rotation angle are illustrated in the following figure:

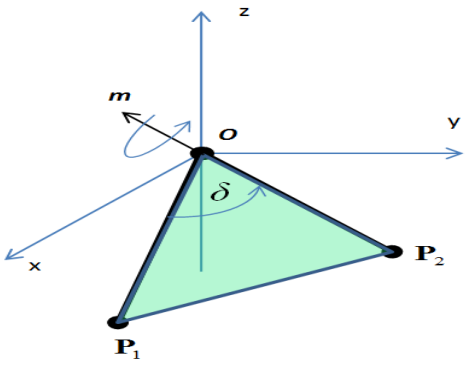

Figure 5: The direct rotation angle δ. $\mathbf{P}_1$ and $\mathbf{P}_2$ are two elbow positions, and ***m*** is a vector normal to the plane defined by points **O**, $\mathbf{P}_1$ and $\mathbf{P}_2$.

The direct rotation angle is calculated by:

$$\delta = \mathrm{Cos}^{-1} \frac{\boldsymbol{P}_1 \cdot \boldsymbol{P}_2}{\|\boldsymbol{P}_1\| \cdot \|\boldsymbol{P}_2\|} \tag{27}$$

and:

$$\delta^2 \neq \left(\theta^{\mathrm{f}} - \theta^{\mathrm{i}}\right)^2 + \left(\eta^{\mathrm{f}} - \eta^{\mathrm{i}}\right)^2 \tag{28}$$

Therefore, the cost function of MAD criterion in this study is formulated as follows:

$$f_{MAD} = \delta^2 + \left(\zeta^{\mathrm{f}} - \zeta^{\mathrm{i}}\right)^2 \tag{29}$$

Since a 4 DOF arm model is redundant by only one DOF, this optimization problem can be solved by a one degree step grid search where solving for the swivel angle that minimizes the cost function under the given constraint, using (29).During the brute force search, the initial posture of the arm remains constant, while the final posture varies with the value of the swivel angle, and the cost function's value changes accordingly.

2.5 Bi-Criterion Model

The JRA and MAD criteria are used independently, as previously explained, to calculate the swivel angles α_{JRA} and α_{MAD},respectively. The synthesized criterion model then merges the two results by calculating the weighted average of the swivel angle $\alpha_{\mathrm{optimal}}$ as defined by:

$$\alpha_{\mathrm{optimal}} = k\alpha_{\mathrm{MAD}} + (1-k)\alpha_{\mathrm{JRA}} \tag{30}$$

where *k*is a weight factor. Its value is later optimized to match experimental results with the model prediction, and to explore its effect on the correlation with the experimental results.

2.6 Pointing Experiment

2.6.1 Subjects Definition

Ten right handed volunteer (ages 22 years to 28 years, heights 1.65 m to 1.93 m, weights 52 Kg to 94 Kg) performed unconstrained point to point movements. None of the participants reported having any clinical symptoms or any history of motor, sensory, or neurological disorders. The subjects were naive as to the purpose the experiment, and were only instructed to perform point to point reaching movement in a natural self-paced way. The experimental protocol was approved by the UCSC IRB committee.

2.6.2 Experimental Setup

Subjects sat on a chair with back rest and adjustable height. They were positioned in front of a spherical target array (see Fig. 6a and Fig. 6b) with a radius of 750 mm, such that the right shoulder was in line with the center of the sphere.The distance between the chair and the target was adjusted for each subject so that his/her elbow flexion angle was approximately 90^0.

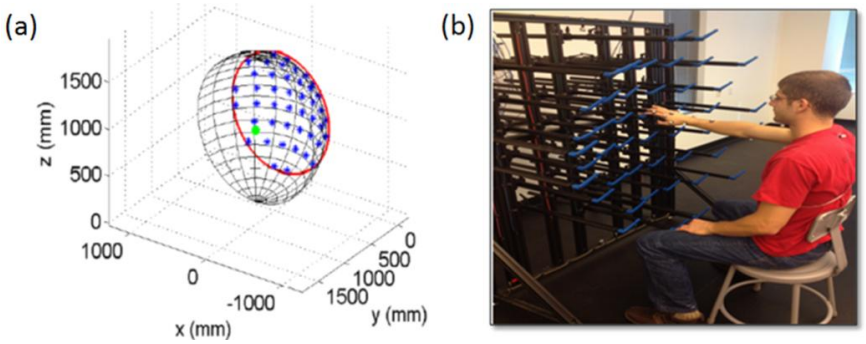

Figure 6: (a) The spherical target array. The stars denote 44 available targets. (b) A subject pointing to a target.

Out of the 44 available targets, eight targets were selected (Fig. 7Figure 7), out of which four (1, 4, 5, and 8) are at boundary of arm's reaching workspace, whereas the remaining four targets are closer to the center of the workspace (2, 3, 6, and 7). Targets consisted of bar ends, retained by a frame, specifically designed for pointing experiments.

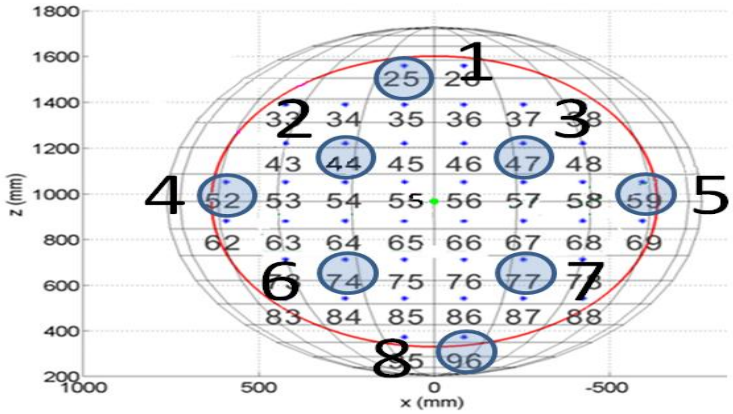

Figure 7: The eight targets used in the pointing experiment, denoted 1 through 8 (large figures).

2.6.3 Experiment Protocol and Data Collection

As part of the experimental protocol the subjects conducted eight sessions of pointing movements with their right arm. Each of the eight sessions consisted of five sets of movements. In each set, subjects started from each one of the seven targets and moved their fingertip to the selected destination target of that set, thus performing seven movements. Fatigue was avoided by resting period between each session. Each subject conducted a total of 280 pointing tasks.

Reflected markers were attached to the human arm and upper body using a standard model. Position of the markers were acquired by a 10 cameras motion capture system (Vicon Motion Systems) at a sampling rate of 100Hz. From experimental sessions, the initial and the final postures of the human arm were identified. Joint angles were calculated off line according to (17)-(20). For each subject, 56 average initial and final postures were calculated.

III. RESULTS

3.1 Experimental Results

Postural invariance of human arm pointing movement was demonstrated in the experiment. Each pointing movement was repeated 5 times. The swivel angle associated with repeated final pointing postures varied in an average range of 8.1^0 with a standard deviation of 4.5^o. This variance is relatively small compared to the variance of average final posture when pointing to all eight targets (68^0 for all subjects). Fig. 8 illustrates the variation of final posture and the effect of initial posture on the final posture for subject 1.

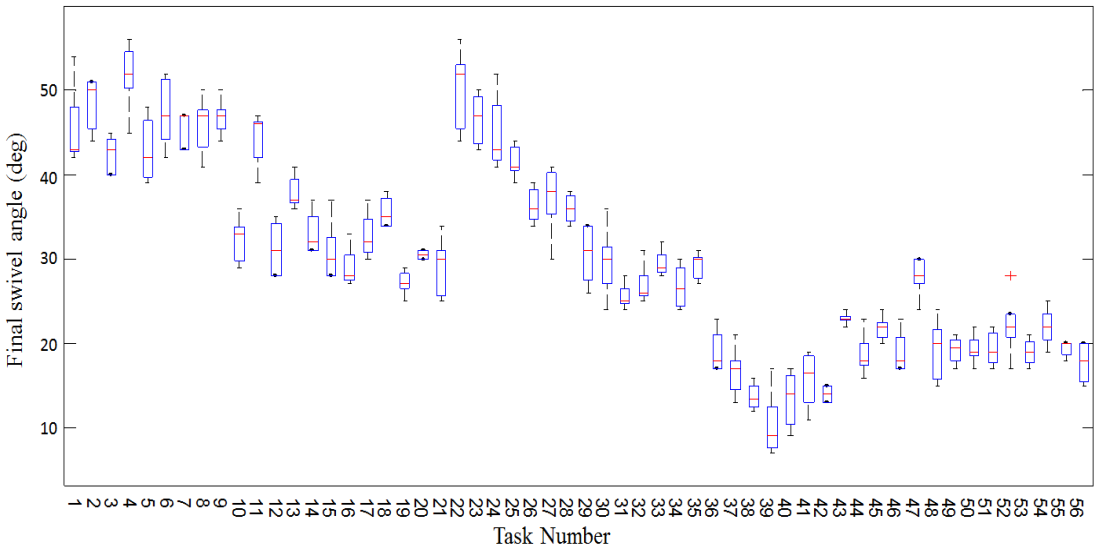

Figure 8: Final posture variability for subject 1.

3.2 MAD model

The correlation between the experimental results and MAD prediction model, using equations (26)is depicted in Fig. 9a. Its trendline slope is 0.5, the offset is 16°, and r^2=0.37. The correlation between the experimental results and MAD prediction model, using equation (29) is depicted in Fig. 9b. Its trendline slope is 0.57, the offset is 14°, and r^2=0.36. These two versions of the MAD model achieved similar results with only a slight advantage for the case of using equation (29).

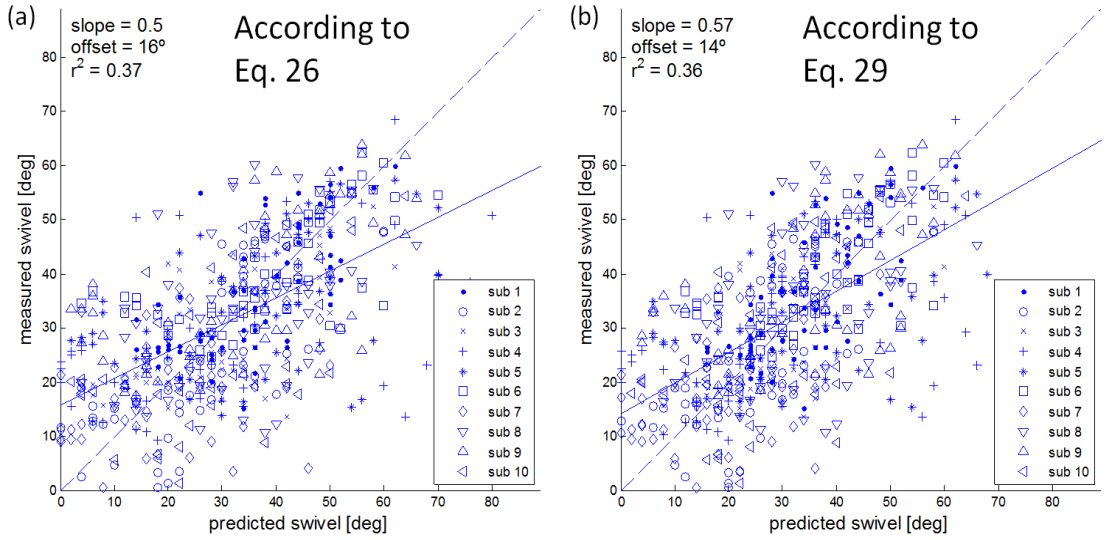

Figure 9: Correlation between experimental results and predictions of MAD model using (26) (a) and (29) (b) for all subjects.

3.3 JRA model

Two alternative definitions for the joint limits were previously defined by equations (23) and (24). Using each of these joint limits resulted in two different arm configurations and associated with two different swivel angles. A typical result expressing these differences is depicted in Fig. 10. The average difference between the two joint limits is 26.2^0 with a standard deviation of 14.4^0.

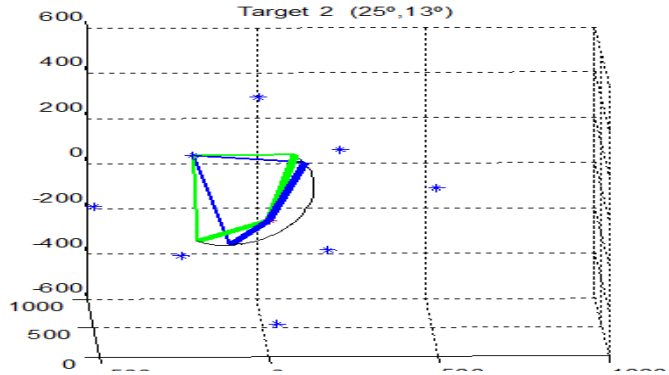

Figure 10: Comparing swivel angle limits according to two different approaches, wheredots represent the targets,thick lines representupper arms,thin lines represent fore-arms,blue lines represent the extremal valid postures found according to (23),green lines represent the extremal valid postures found according to (24),the arc represents the trajectory of the elbow between swivel extremes, andthe numbers in the brackets indicate the differences between the two approaches for pointing to target 2.

The variation in final swivel angle for the spherical surface passing through the targets is depicted in Fig. 11. Uncolored areas in Fig. 11represent unreachable positions due to either being too far from the shoulder (compared to the total arm length), or requiring an elbow flexion angle greater than 150° which occurs in the vicinity of the shoulder. Occlusion of the fingertip with the body is ignored in this simulation.

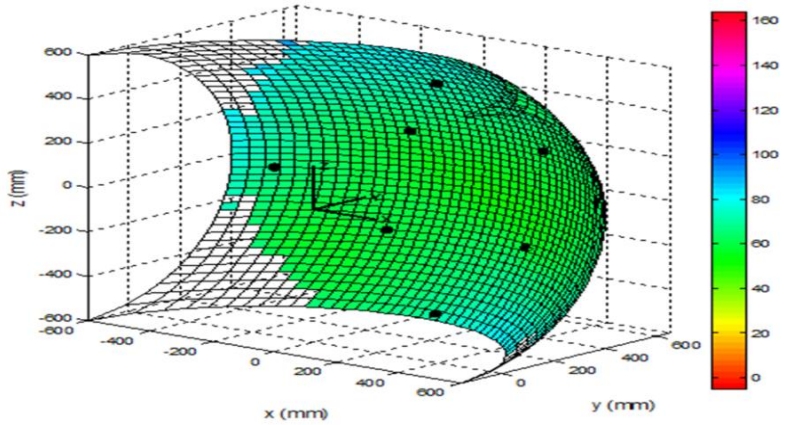

Figure 11: Variation in final swivel angle predicted by the JRA criterion as a function of target position for the spherical surface containing the targets (black dots).

The correlation between the experimental results and JRA prediction model, using equations (23) has a trendline slope of 0.91, an offset of -28° and r^2=0.27, whereas using equation (24) showed a stronger correlation, with a trendline slope of 0.84, an offset of -1° and r^2=0.45. These correlations are depicted in Fig. 12a andFig. 12b, Respectively.

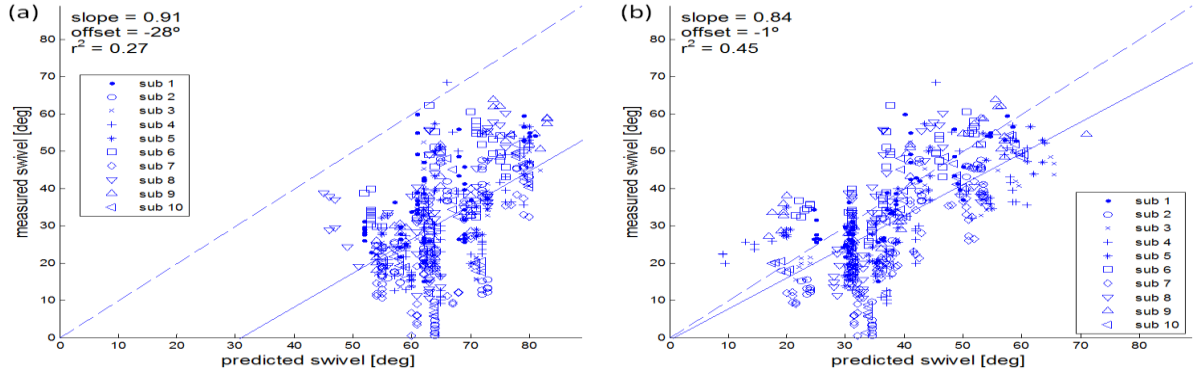

Figure 12: Correlation between experimental results and Predictions of JRA model for all subjects (a) using (23), and (b) using (24).

3.4 Bi-criterion model

The bi-criterion model requires a selection for the weight factor *k*. Three approaches for selecting the weight factor *k*: (1) objective sum, in which *k*=0.5, as suggested in[20][20]; (2) optimizing *k* for highest value of r^2; and (3) optimizing *k* for best trendline slope of unity.

For the bi-criterion model, MAD and the JRA criteria utilized equations (29) and (24) respectively. The correlation between the experimental results and bi-criterion model predictions with a weight factor *k*=0.5, has a trendline slope of 0.88, an offset of 1° and r^2=0.52 as depicted in Fig. 13.

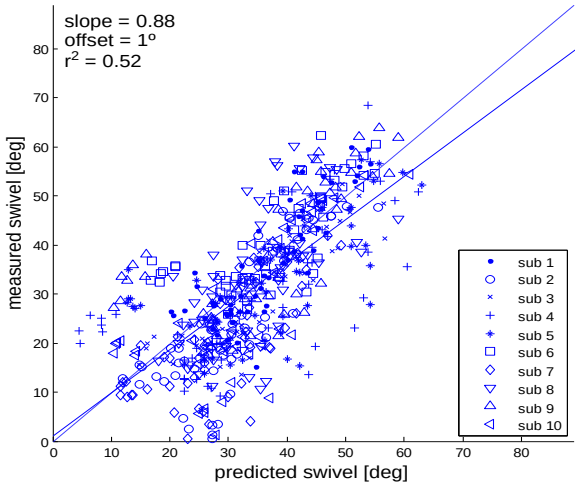

Figure 13: Correlation between experimental results and Predictions of the combined model, where *k*=0.5 (objective sum), for all subjects.

The effect of the weight factor value (*k*) on the trendline slope and on r^2 is depicted in Fig. 14. The highest value of slope (0.29) was achieved with *k*=0.29, and the highest value of r^2=0.54 was achieved with *k*=0.35. Utilizing the objective sum approach (*k*=0.5) yielded a slope of 0.88 and r^2=0.82.

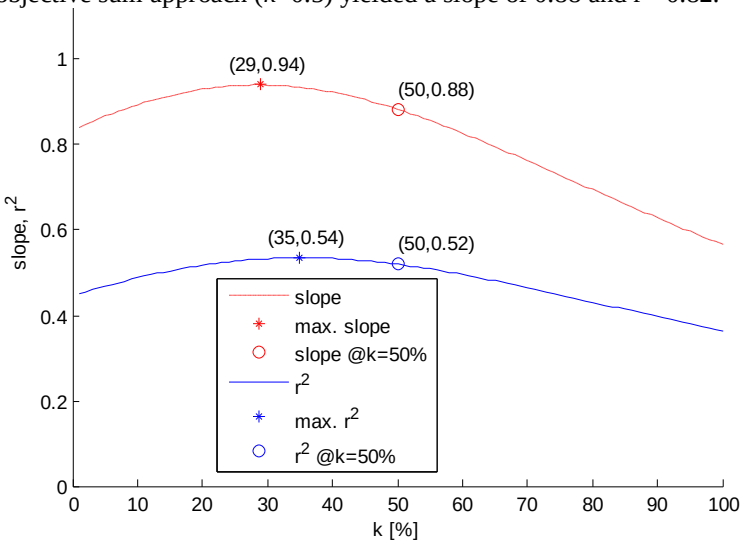

Figure 14: The effect of the weight factor value (*k*) on the trendline slope (dashdot) and on r^2(solid line) for the bi-criterion model combining MAD and JRA criteria. The numbers in parentheses are *k* and slope or r^2.

IV. DISCUSSION

The focal point of this reported research effort is modeling synthesis approach for redundancy resolution of the human arm in pointing tasks. Results for the single criterion models (MAD and JRA) and for the bi-criterion model are presented in table I:

Table I: Single and bi-criterion models results

Model	**Method**	***K***	**Slope**	**offset**	**r^2**
MAD	Eq. (26)		0.5	16^0	0.37
MAD	Eq. (29)		0.57	14^0	0.36
JRA	Eq. (24)		0.84	-1^0	0.45
JRA	Eq. (23)		0.91	-28^0	0.27
MAD+JRA	Objective sum	0.5	0.88	1^0	0.52
MAD+JRA	Optimal slope	0.29	0.94	-3^0	0.53
MAD+JRA	Optimal r^2	0.35	0.92	-2^0	0.54

For a 4 DOF model of the human arm, where there is only one redundant DOF, the synthesized model using two criteria provided higher correlation with our experimental data, compared to results achieved by two single criterion models.

Utilizing the MAD criterion with the direct rotation angle using (29) showed only a minor improvement in the correlation, compared to utilizing it with (26).Swivel angle limits that were calculated according to (23) were found to differ significantly (average 26.2^0) from those calculated according to (24). However, using the more realistic description of the shoulder motion range [18], where the joint limits are co-dependent, did not improve the correlation given the current experimental data. Since the correlation of the JRA model using (23) had a large trendline offset (-28^o), this result is not surprising. The large trendline offset may be associated with fact that (23) allows a larger medial torsion range (up to 97^o) than (24) (up to 220^o), as illustrated in Fig. 15.

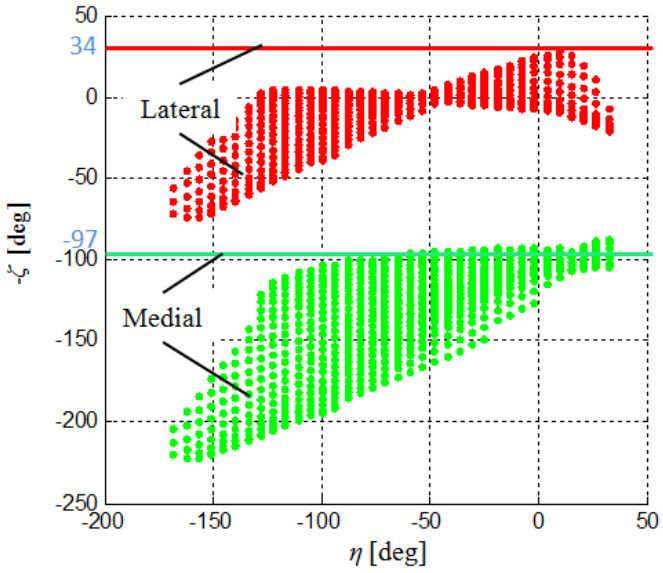

Figure 15: Comparison between humeral torsion range according to (23) (surfaces) and according to (24) (straight lines).

Although the JRA model, using (24) had a relatively close to unity trendline slope, and a relatively high r^2, it cannot be considered to be a good prediction model due to the fact that it is a posture based model, which does not account for the effect of initial posture on the final posture. Other single criterion models shown in Table I had relatively low slope or low r^2. Therefore, it may be deduced that synthesizing the two criteria achieves better correlation given the current experimental data, compared to the correlation with the predictions of single criteria (MAD or JRA) even with the objective sum approach, which does not optimize the weight factor to match the experimental data.

Previous research efforts indicated that correlation of alternative criteria such as the minimal work and minimal torque change were associated with a slope of 0.3 and r^2=0.56 for both criteria [5]. Using the minimum peak kinetic energy criterion[4] led to correlation with slope of approximately 1 and r^2 in the range of 0.522 to 0.915 using a database of four subjects.

Future work will focus on examining the various approaches for integrating criteria (objective sum, min-max, and global sum), and on finding an optimal combination of several criteria to achieve good correlation with experimental data.

Redundancy resolution of articulated serial mechanism such as human or robotic arm has applications in the field of wearable robotics [21,22], where the robot and human body are physically coupled and the need to implement a redundancy resolution algorithm into the control system of the robot is essential to guarantee natural integration between the two systems. Additional application that may benefit for a solution the problem under study might be simulations in ergonomics and computer graphics.

REFERENCES

[1] A.P. Georgopoulos, J.F. Kalaska, and J.T. Massey, Spatial Trajectories and Reaction-Times of Timed Movements – Effects of Practice, Uncertainty, and Change in Target Location, Journal of Neurophysiology, 46, 1981, 725–743.

[2] J.F. Soechting and F. Lacquaniti, Invariant Characteristics of a Pointing Movement in Man, Journal of Neuroscience, 1, 1981, 710–720.

[3] J.F. Soechting, C.A. Buneo, U. Herrmann and M. Flanders, Moving Effortlessly in 3-Dimensions – Does Donders-Law Apply to Arm Movement, Journal of Neuroscience, 15, 1995, 6271–6280.

[4] A. Biess, D.G. Liebermann and T. Flash, A Computational Model for Redundant Human Three-Dimensional Pointing Movements: Integration of Independent Spatial and Temporal Motor Plans Simplifies Movement Dynamics, The Journal of Neuroscience, 27, 2007, 13045-13064.

[5] M.A. Admiraal, M.J. Kuster and S. Gielen, Modeling Kinematics and Dynamics of Human Arm Movements, Motor Control, 8, 2007, 312-338.

[6] Y. Uno, M. Kawato, and R. Suzuki, Formation and Control of Optimal Trajectory in Human Multijoint Arm Movement – Minimum Torque-Change Model, Biological Cybernetics, 61, 1989, 89-101.

[7] E.S. Jung, D. Kee and M.K. Chung, Upper Body Reach Posture Prediction for Ergonomic Evaluation Models, International Journal of Industrial Ergonomics, 16, 1995, 95-107.

[8] Z. Mi, J. Yang and K. Abdel-Malek, Optimization-Based Posture Prediction for Human Upper Body, Robotica, 27, 2008, 607–620.

[9] E.S. Jung, J. Choe and S.H. Kim, Psychophysical Cost Function of Joint Movement for Arm Reach Posture Prediction, Proc. of the Human Factors and Ergonomics Society 38th Annual Meeting, 636-640, 1994.

[10] D.E. Whitney, Resolved Motion Rate Control of Manipulators and Human Prostheses, IEEE Transactions on Man-Machine Systems, 10, 1969, 47-53.

[11] R.T. Marler, J. Yang, J.S. Arora, and K. Abdel-Malek,Study of Bi-Criterion Upper Body Posture Prediction using Pareto Optimal Sets, Proc. of the Fifth IASTED International Conference, 229-234, 2005.

[12] P. Vetter, T. Flash, D.M. Wolpert, Planning Movements in a Simple Redundant Task,Curr. Biol., 12, 2002, 488–491.

[13] T. Okadome, and M. Honda, Kinematic Construction of the Trajectory of Sequential Arm Movements, Biol. Cybern., 80, 1999, 157-169.

[14] F. Hermens, and S. Gielen, Posture-Based or Trajectory-Based Movement Planning: a Comparison of Direct and Indirect Pointing Movements, Exp. Brain Res., 159, 2004, 340–348.

[15] D. Tolani, A. Goswami, and N. I. Badler, Real-Time Inverse Kinematics Techniques for Anthropomorphic Limbs, Graphical Models, 62, 2000, 353-388.

[16] Engin, A.E. and Chen S.M., Statistical Data Base for the Biomechanical Properties of the Human Shoulder Complex—I: Kinematics of the Shoulder Complex, Journal of Biomechanical Eng., 1986.

[17] X. Wang, M. Maurin, F. Mazet, N.D.C. Maia, K. Voinot, J.P. Verriest, and M. Fayet, Three-Dimensional Modeling of the Motion Range of Axial Rotation of the Upper Arm, Journal of Biomechanics, 31, 1998, 899-908.

[18] Chaffin, Andersson, and Martin, Occupational Biomechanics, Wiley, 1984.

[19] J. Rosen and J.C. Perry, Upper Limb Powered Exoskeleton,Journal of Humanoid Robotics, 4, 2007, 1–20.

[20] J. Yang, T. Marler, and S. Rahmatalla, Multi-objective optimization-based method for kinematic posture prediction:development and validation, Robotica, 29, 2011, 245-253.

[21] J. C. Perry, J. Rosen, and S. Burns, Upper-Limb Powered Exoskeleton Design, IEEE Transactions on Mechatronics, 12(4), 2007, 408-417.

[22] H. Kim, L. M. Miller, A. Al-Refai, M. Brand, and J. Rosen, Redundancy Resolution of a Human Arm for Controlling a Seven DOF wearable Robotic System,33rd Annual International Conference of the IEEE Engineering in Medicine and Biology Society (EMBC), Boston MA, 2011.